

EFFECT OF SURFACE FUNCTIONAL GROUPS ON WATER VAPOR ADSORPTION OF EUCALYPTUS WOOD-BASED ACTIVATED CARBON

Yuvarat Ngernyen¹, Chaiyot Tangsathitkulchai^{1*}, Sumet Khaoya¹, Wasan Intasa-ard¹ and Malee Tangsathitkulchai²

Received: Aug 22, 2006; Revised: Jan 8, 2007; Accepted: Jan 16, 2007

Abstract

The aim of this study is to modify activated carbon surfaces by oxidizing them with HNO₃ to enhance the adsorption capacity of water vapor. The activated carbons were prepared from eucalyptus wood by CO₂ activation at 600°C and 900°C, giving activated carbons with different porous properties. The results from Boehm titration showed that the amount of acidic oxygen functional groups increased after oxidation with HNO₃ for both activated carbons, with activated carbon prepared at 900°C giving the higher amount of acidic oxygen functional groups. The activated carbon originally prepared at 900°C gave higher amounts of water adsorbed than the carbon prepared at 600°C because of its larger pore volume and surface area. The adsorption capacity of water vapor was found to increase after oxidation for both activated carbon samples. Water isotherms were also analyzed using the cluster model of Dubinin-Serpinski (DS) and Do and Do. The results indicated that water isotherms obtained from the original and oxidized activated carbons prepared at 600°C were well described by the Do and Do model over the relative pressure close to unity. However, the water isotherms of the original and oxidized activated carbons prepared at 900°C could only be described by the Do and Do model when the cluster size in the model was increased for adsorption in the high relative pressure range.

Keywords: Activated carbon, eucalyptus wood, surface functional groups, adsorption, water vapor

¹ School of Chemical Engineering, Institute of Engineering, Suranaree University of Technology, Nakhon Ratchasima, 30000, Tel: 0-4422-4490, Fax: 0-4422-4609, E-mail: chaiyot@g.sut.ac.th

² School of Chemistry, Institute of Science, Suranaree University of Technology, Nakhon Ratchasima, 30000

* Corresponding author

Introduction

Activated carbon is a carbonaceous adsorbent with a highly porous structure. It is used in a wide range of applications which are concerned with the removal of species by adsorption from the liquid or gas phase to purify, store or recover the chemicals (Girgis *et al.*, 2002). Activated carbon is the most widely used adsorbent because of its large adsorptive capacity and low cost. The adsorption property of activated carbon depends on its surface chemistry and internal porous structure (Gomez-Serrano *et al.*, 1996). Basically, activated carbon contains hydrophobic graphene layers and associated surface functional groups which can impart some hydrophilic characteristic, thus enabling the increase of adsorption capacity for a specific or polar adsorbate in the gaseous or liquid phase. Surface oxygen functional groups can be additionally introduced on activated carbon surfaces when they are treated with oxidizing solutions such as HNO_3 , H_2O_2 and $(\text{NH}_4)_2\text{S}_2\text{O}_8$ or gases such as air and O_3 . In general, the order of the extent of oxidation produced is $\text{HNO}_3 > \text{H}_2\text{O}_2 > \text{air}$ (El-Hendawy, 2003). This treatment introduces two types of oxygen functional groups i.e. acidic and basic (Moreno-Castilla *et al.*, 2000). Examples of acidic oxygen functional groups are carboxyl, lactone, and phenol while carbonyl, ether and chromene are typical of the basic character. The surface acidity of activated carbon is of importance in improving the adsorption uptake of the polar adsorbates such as water vapor and methanol (Salame and Bandosz, 2000) and adsorbates with a positive charge such as Cr(III) (Cordero *et al.*, 2002) and Cu(II) (Biniak *et al.*, 1999) ions in solutions.

The presence of water vapor in the air or gas streams containing contaminants is known to decrease the breakthrough time for the activated carbon bed, and hence deteriorates the adsorption performance of the activated carbon bed (Harding *et al.*, 1998). It is generally accepted that both the surface chemistry and porous structure of activated carbon can play an important role on the behavior of water vapor adsorption (Vagner *et al.*, 2002). The most well-known model for water adsorption was proposed

by Dubinin and Serpinsky (DS) (Dubinin and Serpinsky, 1981). The description of water isotherms is based on the interaction of water molecules with oxygen functional groups present on the activated carbon surface. The DS model assumes that water is first adsorbed on primary adsorption sites (functional groups containing oxygen) followed by adsorption on secondary sites (adsorbed water molecules) via hydrogen bonding (Salame and Bandosz, 1999). Later, Do and Do (2000) presented another model for describing the adsorption equilibrium of water vapor on activated carbon. This model is based on the growth of the water cluster at the surface functional groups followed by the transport of water clusters into the micropore in the form of pentamer (five water molecules). This model is able to describe most of water adsorption behaviors of non-polar surface activated carbon as well as highly oxidized activated carbon. Presently, the molecular simulation using a grand canonical Monte Carlo model is gaining increasing acceptance as a tool to study water adsorption phenomena at a molecular level. The results obtained from Müller *et al.* (1996); McCallum *et al.* (1999), and Birkett and Do (2006) revealed that the density and strength of oxygen surface functional groups and the pore width had a direct effect on water adsorption behavior.

The objective of this study is to modify the surface of eucalyptus wood-based activated carbon with HNO_3 to enhance the adsorption capacity of water vapor. The surface chemistry of the test carbons was characterized by the Boehm titration technique and the carbon porous properties were assessed by N_2 adsorption to examine the effect of incorporation of oxygen functional groups on the porous structure of activated carbons. The water isotherms were measured and analyzed using the cluster models proposed by Dubinin-Serpinski and Do and Do.

Materials and Methods

The original activated carbons were prepared

from eucalyptus wood chip obtained from a local sawmill. The wood chip was milled and sieved to obtain the size fraction of 20 x 30 mesh (average size of 0.714 mm). About 7 g of the sieved fraction was carbonized at 400°C for 1 h in a tube furnace (Model CTF12/75/700/201, Carbolite) under the constant flow of N₂ (100 cm³/min). The char derived from the carbonization step (~ 3 g) was further activated in a packed-bed reactor (2.5 cm diameter and 10 cm long) placed inside a tube furnace under the constant supply of a gas mixture of CO₂ (100 cm³/min) and N₂ (100 cm³/min), giving 50% CO₂ by volume in the gas mixture. The activation step was carried out at 600°C and 900°C for 1 h, giving activated carbons with char burn-off of 21% and 83%, respectively. Based on our previous work (Ngernyen *et al.*, 2006) on the preparation of activated carbons from eucalyptus wood, two activation temperatures (600°C and 900°C) were selected to produce activated carbons with two different porous structures so that the effect of pore size distribution on the variation of surface groups and subsequent water adsorption behavior could be studied. The activated carbons prepared at 600°C and 900°C were designated as AC600 and AC900, respectively.

The oxygen functional groups were incorporated on the activated carbon surfaces by oxidation with 1 M HNO₃. The experiment was performed by boiling the activated carbon samples in a reflux condenser for 24 h. After oxidation, the oxidized activated carbons were washed with water in a Soxhlet apparatus to remove excess oxidizing agent and other water-soluble species. The activated carbons oxidized with HNO₃ were designated as AC600-HNO₃ and AC900-HNO₃.

The type and concentration of surface functional groups of activated carbons was determined by the Boehm titration technique (Salame and Bandosz, 2003). This technique assumes that the following surface functional groups become neutralized as follows: carboxylic groups in a solution of NaHCO₃, carboxylic and lactonic groups in a solution of Na₂CO₃ and carboxylic, lactonic, and phenolic groups in a solution of NaOH. The basic groups on the

activated carbon surface were determined based on the neutralization with HCl. The procedure commenced by loading about 1 g of the activated carbon into each of the 100 cm³ of 0.1 M solutions of HCl, NaOH, NaHCO₃ and 0.05 M Na₂CO₃, respectively. The vials were sealed and shaken for 24 h, and the activated carbon suspensions were filtered. The remaining solutions of NaHCO₃, Na₂CO₃ and NaOH were pipetted and titrated with 0.1 M HCl while the remaining solution of HCl was titrated with 0.1 M NaOH. The consumptions of the various bases and acid were used to determine the amount of functional groups on the activated carbon surface. It should be noted that the Boehm titration for determining the amounts and types of surface functional groups on activated carbon has been widely used by many researchers (Strelko *et al.*, 2002; Jiang *et al.*, 2003; Rivera-Utrilla and Sánchez-Polo, 2003). Total surface acidity values determined in this work are comparable to those reported by the previous workers.

The specific surface area and pore volume of the original and oxidized carbons were determined using N₂ gas adsorption data at -196°C obtained by employing an automated adsorption apparatus (Model ASAP 2010, Micromeritics, USA). The specific surface area was estimated by applying the Brunauer-Emmett-Teller (BET) equation to the isotherm data (Do, 1998). The micropore volume was calculated by using the Dubinin-Radushkevich (DR) equation (Do, 1998). The total pore volume was found from the amount of N₂ gas adsorbed at the relative pressure of 0.99 and converting it to the corresponding volume of liquid state. The volume of mesopore and macropore was found from the difference between total pore volume and micropore volume. The average pore width was calculated via the equation $4V_T/A$, where V_T is the total pore volume and A is the BET surface area. Pore size distributions were also computed by applying the Density Functional Theory (DFT) to the isotherm data (Olivier, 1995).

In studying water vapor adsorption of the original and oxidized activated carbons, an Intelligent Gravimetric Analyzer (Model IGA

002, Hiden Analytical, UK) was used. This apparatus (Figure 1) is fully computer controlled and measures the amount of water adsorbed via a microbalance. Prior to the adsorption measurement, the activated carbon was first outgassed at 250°C at least for 5 h until the weight became constant, at a vacuum pressure. The liquid used to generate the vapor was degassed fully by repeated evacuation of the liquid reservoir. The adsorption was studied over the relative pressure range from 0–0.94 at 30°C. The sample temperature was maintained by a thermostat and sample chamber jacket. The mass uptake was measured as a function of time, and after equilibrium was established, the pressure was increased to the next set pressure value and the subsequent uptake was measured until equilibrium was re-established.

Results and Discussion

Activated Carbon Properties

The proximate analysis and lignocellulosic composition of the eucalyptus wood sample are shown in Table 1. The results show that eucalyptus wood has a fixed carbon content of 18.3%, and contains a high proportion of volatile matter but with low ash content. Table 1 also shows that eucalyptus wood has a cellulose content of 57.3%, hemicellulose content of 16.8%, and lignin content of 25.9%. According to Jagtoyen and Derbyshire (1998), hardwoods have a cellulose content of about 52%, a hemicellulose content of about 14–25% and a lignin content of about 25–34%. Therefore, the eucalyptus wood used in this study is classified as a hardwood type.

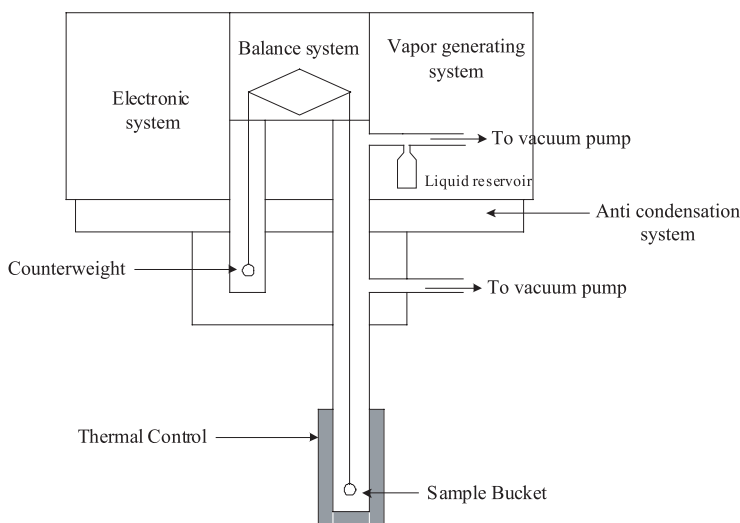


Figure 1. Diagrammatic of intelligent gravimetric analyzer for adsorption experiment

Table 1. Proximate analysis and lignocellulosic composition of eucalyptus wood

| Proximate analysis (wt%) | | | | Lignocellulosic composition (wt%) | | |
|--------------------------|------------------|-----|----------|-----------------------------------|---------------|--------|
| Fixed carbon | Volatile matters | Ash | Moisture | Cellulose | Hemicellulose | Lignin |
| 18.3 | 76.4 | 1.2 | 4.1 | 57.3 | 16.8 | 25.9 |

The porous properties of the original and oxidized activated carbons are shown in Table 2. The results show that for the original activated carbons the increase in activation temperature from 600°C to 900°C leads to an increase in BET surface area, total pore volume, volume of all pore sizes, as well as the average pore width. The improvement in porous properties of carbons is undoubtedly caused by the increase in the extent of the gasification reaction of CO₂ with the carbon mass, as reflected by increased char burn-off from 21 to 83% (as noted in the section of Materials and Method). The results also indicate that the prepared activated carbons developed mainly micropore structure (pore size < 20 Å). There is the tendency that the percentage of micropore volume decreases (91% to 82%) with the increase in activation temperature from 600°C to 900°C. As the activation temperature is increased new micropores are developed by C–CO₂ reaction as well as the widening of original micropores due to the gasification reaction and possibly the collapse of adjacent pore walls leading to the formation of mesopores and macropores. As a result of this pore development, larger pores are created at the expense of smaller pores and hence a decrease in the proportion of micropore volume. Figure 2 shows the pore size distributions in discrete and cumulative form of both original activated carbons derived by

applying the Density Functional Theory (DFT). Both activated carbons contain predominantly micropores (< 20 Å). The curves show the main peak of pore size distribution around 7 Å for both carbons. The second smaller peaks occur at 5 Å for carbon prepared at 600°C and 12 Å for carbon prepared at 900°C. According to Lastoskie *et al.* (1993) the micropore can be further subdivided into ultramicropore (pore size ≤ 7 Å) and supermicropore (pore size 7 – 20 Å). The curves also show that the micropore volume (pore size smaller than 20 Å) present in the carbon prepared at 900°C is higher than that of carbon prepared at 600°C, which is in agreement with micropore volume (determined independently using DR equation) reported in Table 2. This confirms that both the original activated carbons possess different pore size distributions. Figure 3 shows the pore size distributions in discrete and cumulative form of the oxidized activated carbon prepared at 900°C (AC900-HNO₃). The results show the smaller of both peaks (at 7 Å and 12 Å) and lower cumulative pore volume of the oxidized activated carbon than those of the original activated carbon (Figure 2), which is also in agreement with the results presented in Table 2. However, data on pore size distribution of AC600-HNO₃ was not shown here since their values are not significantly different from the original carbon (AC600).

Table 2. Porous characteristics of activated carbons obtained from N₂ adsorption isotherm

| Samples | BET surface area (m ² /g) | Micropore volume (cm ³ /g) | Meso- and macropores volume (cm ³ /g) | Total pore volume (cm ³ /g) | Average pore width (Å) |
|------------------------|--------------------------------------|---------------------------------------|--|--|------------------------|
| AC600 | 460 | 0.21 (91%) | 0.02 (9%) | 0.23 (100%) | 20.0 |
| AC600-HNO ₃ | 405 | 0.20 (87%) | 0.03 (13%) | 0.23 (100%) | 22.7 |
| AC900 | 1,491 | 0.66 (82%) | 0.14 (18%) | 0.80 (100%) | 21.5 |
| AC900-HNO ₃ | 1,161 | 0.50 (74%) | 0.18 (26%) | 0.68 (100%) | 23.4 |

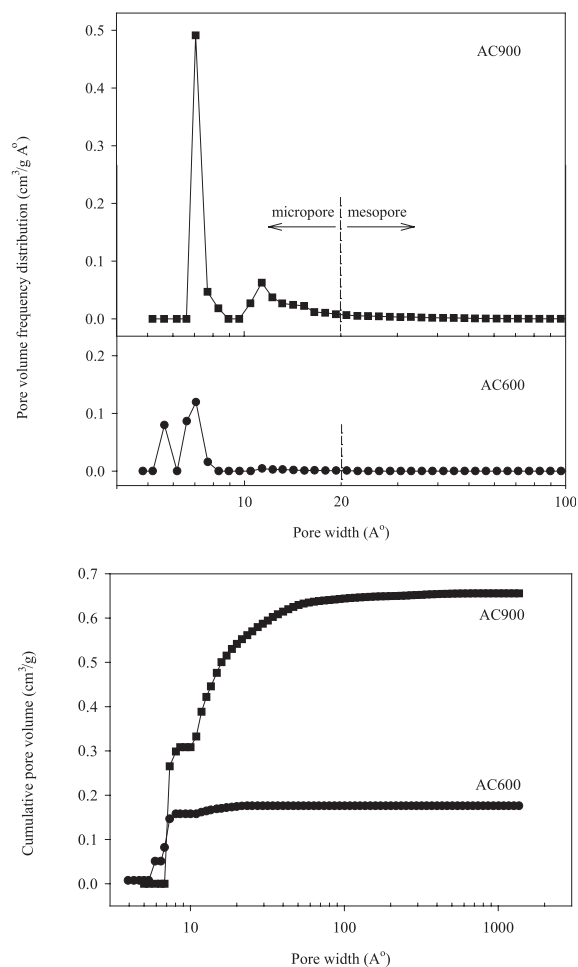


Figure 2. Pore size distribution of original activated carbons prepared by CO_2 activation at (a) 900°C and (b) 600°C in discrete and cumulative form

The values of the acidic and basic groups determined from Boehm titration are shown in Table 3. The original activated carbon prepared at 900°C (AC900) had higher amounts of acidic and basic groups as compared to the carbon prepared at 600°C (AC600). It appears that before oxidation each carbon sample shows the highest concentration of the phenolic ($-\text{OH}$) group for the acidic surface functionality. The AC900 sample contains a notably higher amount of the phenolic group but gives comparable amounts of the carboxylic ($-\text{COOH}$) and lactonic ($-\text{COO}$) groups on the carbon surfaces. After oxidation, the total acidic groups increase for

both of the original carbons. In view of the three acidic groups, the maximum increase in concentration after oxidation occurs with the carboxylic group (450% for AC600 and 700% for AC900). It is also observed that after being oxidized with HNO_3 both carbon samples contain the highest proportion of the carboxylic group. It is further noted that the basic groups also increase after oxidation. This increase in the basic groups could arise from the presence of nitrate or nitro surface groups introduced by HNO_3 oxidation (Haydar *et al.*, 2003). Salame and Bandosz (2001) proposed two distinct mechanisms of nitric acid interacting with the

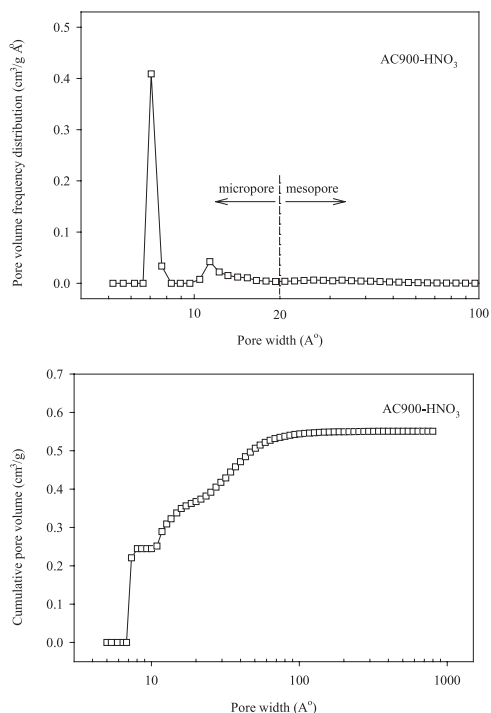


Figure 3. Pore size distribution of oxidized activated carbons prepared at 900°C in discrete and cumulative form

Table 3. Boehm titration results in mmol/g

| Samples | Acidic groups | | | | Basic group |
|------------------------|---------------|---------------|---------------|----------------|-------------|
| | Carboxylic | Lactonic | Phenolic | Total | |
| AC600 | 0.20 (17%) | 0.36 (30%) | 0.64 (53%) | 1.20 (100%) | 0.40 |
| AC600-HNO ₃ | 1.10 (56%) | 0.52 (26%) | 0.36 (18%) | 1.98 (100%) | 0.60 |
| AC900 | 0.16 (10%) | 0.38 (24%) | 1.06 (66%) | 1.60 (100%) | 1.17 |
| AC900-HNO ₃ | 1.29 (60%) | 0.75 (34%) | 0.13 (6%) | 2.17 (100%) | 1.58 |

activated carbon surface i.e. oxidative and nitrate routes. In the oxidative route, oxygen functional groups are introduced to the activated carbon surface while nitration introduces nitro groups to the activated carbon surface.

The results from Table 2 show that the specific surface area and micropore volume of oxidized activated carbons decrease as compared

with the original activated carbons. This is probably caused by the inaccessibility of N₂ molecules to the adsorption sites due to the obstruction of increased surface oxygen functional groups, which are formed at the pore entrance, and possibly by the destruction of some thin pore walls, as detected by the increase in the average pore size shown in Table 2.

Water Adsorption Behavior

The water vapor adsorption and desorption isotherms of the original and oxidized activated carbons are shown in Figure 4. These isotherms are of Type V (Type III plus hysteresis loop) according to the IUPAC classification (Rouquerol *et al.*, 1999). These hystereses exist as the result of differences in pore filling (adsorption) and emptying (desorption) mechanisms. It is observed that the hystereses do not close until at a very low relative pressure. This may arise from the difficulty in breaking the hydrogen bonds which give strong adsorption between water molecules and surface functional groups (Rouquerol *et al.*, 1999). Moreover, the size of the hysteresis loop of the

original activated carbons increases with an increase in activation temperature. This trend agrees with the average pore width which also increases with an increase in activation temperature. Thus, it can be concluded that the size of the hysteresis loop correlates reasonably with the average pore width. The mechanism of the pore emptying involves the removal of adsorbed molecules existing as a stable phase in pores which would be more liquid-like phase in the central layers as the pore width is increased. Thus, the desorption process in large pores is difficult to remove from the adsorbed phase (Rouquerol *et al.*, 1999). This should explain why the activated carbon activated at a high temperature has a larger hysteresis size than the carbon activated at the lower temperature.

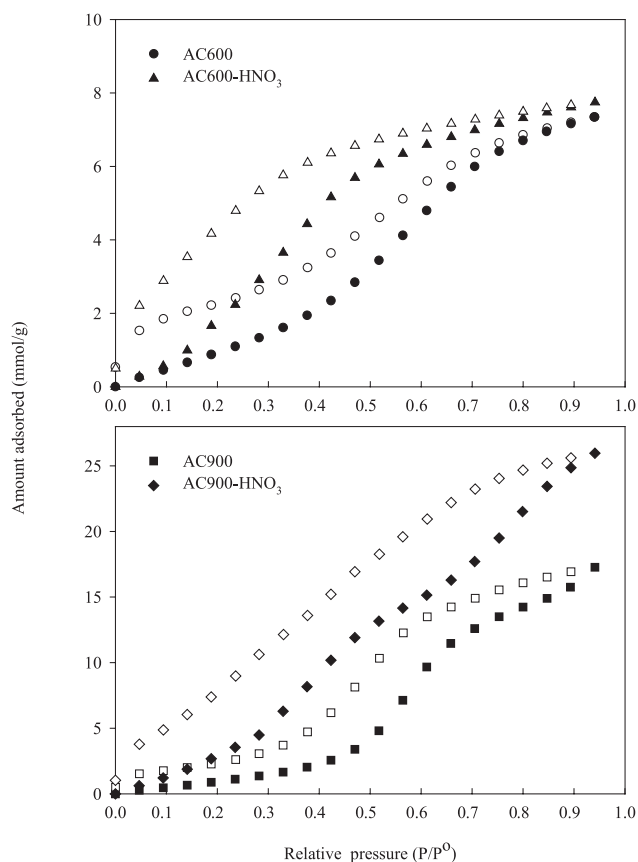


Figure 4. Water vapor adsorption and desorption isotherms of original and oxidized activated carbons at 30°C: Closed symbols adsorption and open symbols desorption

The adsorption behavior of the original (AC600 and AC900) and oxidized (AC600-HNO₃ and AC900-HNO₃) activated carbons is further examined by replotting only the adsorption branches of the isotherms, as displayed in Figure 5. It should be emphasized that the main mechanism of water adsorption is by the adsorption of the first water molecule on the acidic functional groups (or acidic sites) followed by cluster formation of additional molecules via hydrogen bonding. The change in porous structure i.e., the variation of surface area and pore volume, will inevitably cause a change in the amount of surface functionalities. The effect of pore size and surface functional groups on water adsorption behavior is therefore difficult to isolate.

In principle, the adsorption should occur first in micropores at low pressure, mainly due to the stronger interaction forces induced by the narrow pore walls, then adsorption proceeds in the larger pores at a higher pressure once the micropores are completely filled with an adsorbate (Rouquerol *et al.*, 1999). Based on this reasoning and on the observation of the isotherm shape of the original carbons in Figure 6, it is proposed that the adsorption of AC600 and AC900 may be arbitrarily divided into three

consecutive ranges of relative pressure: 0 – 0.3, 0.3 – 0.8, and 0.8 – 0.9, corresponding to adsorption into ultramicropore (pore size $\leq 7 \text{ \AA}$), supermicropore (pore size 7 – 20 \AA) and mesopore (pore size $> 20 \text{ \AA}$), respectively. Table 4 shows this adsorption behavior. As Figure 6 shows, the amount of water adsorbed over the relative pressure of 0 – 0.3 increases approximately linearly with pressure and is the same for AC600 and AC900. This behavior can be explained in part by the fact that both carbons contain the same volume of ultramicropore (Figure 2) as shown in Table 4 and perhaps the same amount of acidic surface groups. In the range of relative pressure 0.3 – 0.8, the amount adsorbed for AC900 still increases steadily while that of AC600 increases but to a much lesser extent due to the lesser volume of larger supermicropore. In the last pressure range of 0.8 – 0.9, AC900 can further adsorb water into the mesopore while there is little change in the amount adsorbed for AC600 which contains almost no mesopore volume. These results may lead to the conclusion that carbon with larger area and volume should contain higher amounts of available surface functional groups, giving rise to higher adsorptive capacity for water.

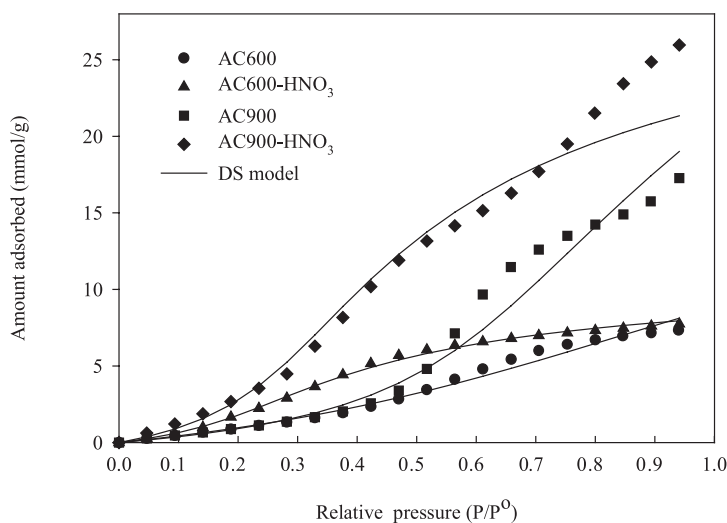


Figure 5. Fitting of the Dubinin-Serpinsky (DS) model to the water vapor adsorption isotherms at 30°C

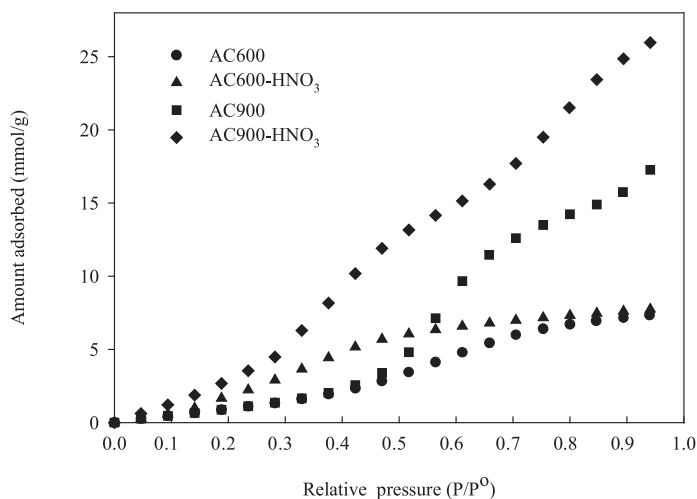


Figure 6. Water vapor adsorption isotherms of original and oxidized activated carbons at 30°C

Table 4. Amount of water adsorbed at various pore sizes

| Pore size (Å) | Actual pore volume (cm ³ /g) | | P/P ⁰ | Amount of water adsorbed (mmol/g) | |
|-----------------------------|--|-------|------------------|--------------------------------------|-------|
| | AC600 | AC900 | | AC600 | AC900 |
| ≤ 7 (ultramicro-pore) | 0.103 | 0.103 | 0 – 0.3 | 1.48 | 1.48 |
| 7 – 20 (supermicro-pore) | 0.071 | 0.439 | 0.3 – 0.8 | 5.22 | 12.75 |
| > 20 (mesopore) | 0.002 | 0.114 | 0.8 – 0.9 | 0.64 | 3.04 |

The results from Figure 6 also indicate that surface oxidation can increase the water vapor uptake over the entire range of pressure for both original activated carbons, emphasizing the important role of surface functional groups. The water uptake of AC600-HNO₃ is higher than that of AC600 up to the relative pressure of about 0.8, above which there is little adsorption for both carbons, possibly caused by the complete consumption of active sites of adsorption available in the micropore volume. The proportional increase of water adsorbed by AC600-HNO₃ appears to be a function of

relative pressure and hence the pore size, with the maximum increase occurring in the relative pressure range of 0.4–0.5. It is believed that the acidic functional groups that participate in water adsorption, possibly the carboxylic group, might not evenly distribute over the pore size range of the oxidized carbon. This behavior is in contradiction to the isotherms of AC900 and AC900-HNO₃ where the adsorption capacity of the latter is proportionally higher than the former over the entire range of relative pressure. It may be inferred that activated carbon containing greater pore volume and

surface area, particularly with some mesopore volume, can provide a higher amount of acidic surface groups which further help to increase the adsorption capacity.

Simulation of Water Isotherms

One of the well-known models for water vapor adsorption on activated carbon is due to Dubinin and Serpinsky (Dubinin and Serpinsky, 1981). The DS equation was first adopted in this study to check the model validity in predicting the water isotherms. The final DS equation is in the form

$$C_{\mu} = \frac{-\frac{1}{k}\left(\frac{1}{cx} + kC_{\mu 0} - 1\right) + \sqrt{\frac{1}{k^2}\left(\frac{1}{cx} + kC_{\mu 0} - 1\right)^2 + \frac{4C_{\mu 0}}{k}}}{2} \quad (1)$$

where C_{μ} is the adsorbed concentration of water in mmol/g, $C_{\mu 0}$ is the concentration of the primary sites in mmol/g, k is the rate of loss of the secondary sites due to the finiteness of the adsorption volume in g/mmol, c is the ratio of the adsorption rate constant and desorption rate constant (k_{ads}/k_{des}) and x is the relative pressure (P/P^0).

Figure 5 shows the fitting of the DS model to the water vapor adsorption isotherms and Table 5 gives the model parameters. The DS model can fit the isotherm of original activated carbon prepared at 600°C better than carbon prepared at 900°C. The model fails to fit the isotherm of carbon prepared at 900°C when the relative pressure is higher than about 0.5, at which a sharp increase of the isotherm curve occurs. After oxidation, the DS model can still describe the isotherm of activated carbon

prepared at 600°C better than carbon prepared at 900°C. Again, the model fails to fit the isotherm of oxidized activated carbon prepared at 900°C when the relative pressure is higher than about 0.5 caused by the inflection nature of the curve. The concentration of the primary sites ($C_{\mu 0}$) predicted from this model gives a higher concentration of acidic functional groups than that determined from Boehm titration for all activated carbons, except for oxidized activated carbon prepared at 600°C which shows a lower concentration of functional groups.

Recently, Do and Do (2000) proposed another cluster model for water vapor adsorption on activated carbon. This model is based on the growth of the water cluster at the surface functional groups and the penetration of water clusters into the micropore in the form of a pentamer that has enough dispersive energy to enter into the micropores. The general form of the Do and Do model is:

$$C_{\mu} = S_0 \frac{K_f \sum_{n=1}^{\infty} nx^n}{1 + K_f \sum_{n=1}^{\infty} x^n} + C_{\mu s} \frac{K_{\mu} \sum_{n=6}^{\infty} x^n}{K_{\mu} \sum_{n=6}^{\infty} x^n + \sum_{n=6}^{\infty} x^{n-5}} \quad (2)$$

where C_{μ} is the water adsorbed concentration in mmol/g, S_0 is the functional group concentration in mmol/g, K_f is the chemisorption equilibrium constant, $C_{\mu s}$ is the saturation concentration in micropore in mmol/g, K_{μ} is the micropore equilibrium constant, n is the number of water molecules in a cluster taken as 5 and x is the relative pressure (P/P^0). The first term of this equation is related to the adsorption on the

Table 5. Parameters obtained from Dubinin-Serpinsky equation

| Samples | $C_{\mu 0}$ (mmol/g) | k (g/mmol) | c | R^2 |
|------------------------|-------------------------|-----------------|------|-------|
| AC600 | 3.97 | 0.04 | 1.01 | 0.984 |
| AC600-HNO ₃ | 1.41 | 0.09 | 3.34 | 0.997 |
| AC900 | 2.29 | 0.02 | 1.44 | 0.968 |
| AC900-HNO ₃ | 2.47 | 0.03 | 2.88 | 0.971 |

R^2 = correlation coefficient

primary sites and the second term corresponds to the adsorption of the pentamer into the micropores. This model separates the contribution of the functional groups from the effect of the microporosity. Thus the total water adsorbed concentration is the sum of that by the functional group and that by micropore filling.

Figure 7 shows the fitting of the Do and Do model to the water vapor adsorption isotherms and Table 6 gives the corresponding model parameters. As shown in Figure 7, the Do and Do model provides a better isotherms fit for AC900 and AC900-HNO₃ as compared with the DS model for all activated carbons. However, it cannot properly account for the inflection characteristic of the curves for carbons prepared at 900°C. The results from Table 6 show that for both original activated carbons and oxidized activated carbon prepared at 600°C the

concentrations of the functional group (S_0) estimated from this model are closer to the values derived from Boehm titration but for the oxidized activated carbon prepared at 900°C these values are much greater than the Boehm titration results.

The work of Junpirom *et al.* (2006) suggested that the original Do and Do model could be improved when simulating the water isotherms for activated carbon containing mesoporosity. Thus, this model was adopted to simulate the water isotherms of the original and oxidized activated carbons prepared at 900°C containing about 20% of mesopore volume. For this modified model, the number of the water molecules in the cluster (n) can be changed from five to an arbitrary number, depending on the range of relative pressure. In this study, the isotherms were divided roughly into two

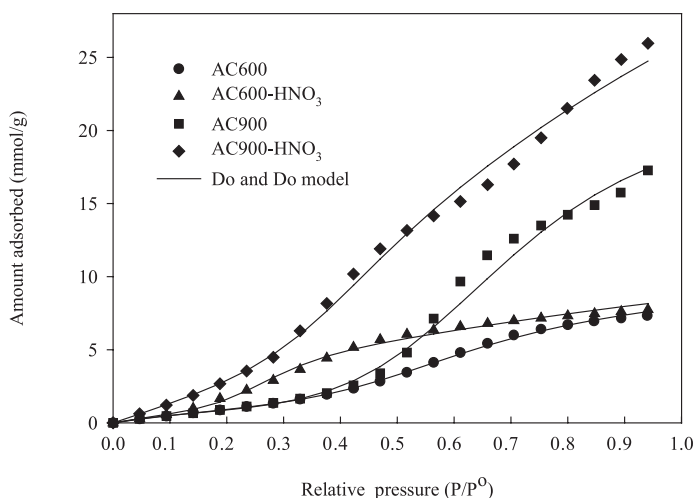


Figure 7. Fitting of the Do and Do model to the water vapor adsorption isotherms at 30°C

Table 6. Parameters obtained from Do and Do model

| Samples | S_0 (mmol/g) | K_f | $C_{\mu s}$ (mmol/g) | K_{μ} | R^2 |
|------------------------|-------------------|-------|-------------------------|-----------|-------|
| AC600 | 1.43 | 4.08 | 4.12 | 12.71 | 0.999 |
| AC600-HNO ₃ | 1.85 | 3.72 | 3.16 | 560.41 | 0.995 |
| AC900 | 1.10 | 6.35 | 17.45 | 6.27 | 0.990 |
| AC900-HNO ₃ | 7.50 | 1.70 | 5.97 | 53.90 | 0.993 |

relative pressure ranges i.e. $P/P^0 \leq 0.5$ and $P/P^0 > 0.5$, the value of which represents the point of curve inflection. The cluster size (n) was determined by a trial and error search procedure to give the best fit between the experimental data and the data predicted by the model.

Figure 8 shows the fitting of the modified Do and Do model to the water vapor adsorption isotherms and Table 7 gives the model parameters. The results show that the modified Do and Do model can fit the experimental data very well over the entire range of relative pressure except at the relative pressure higher than 0.9 where the effect of capillary condensation might occur (Do and Do, 2000). The original activated carbon (AC900) shows

the inflection point at the relative pressure of 0.5 with 5 and 10 water molecules in a cluster for adsorption at relative pressure lower and higher than 0.5, respectively. The inflection point of oxidized activated carbon (AC900-HNO₃) was found to be 0.5 with the cluster size being 5 and 15 for the lower and higher relative pressure range, respectively. The difference in the cluster size of both carbons is possibly ascribed to the difference in their porous structure. The increasing cluster size for the high relative pressure range, where the adsorption occurs in the mesopores and macropores, is the result of the lower interaction energy of solid surface and adsorbate molecules in mesopores as compared with that in the micropores (Junpirom *et al.*, 2006).

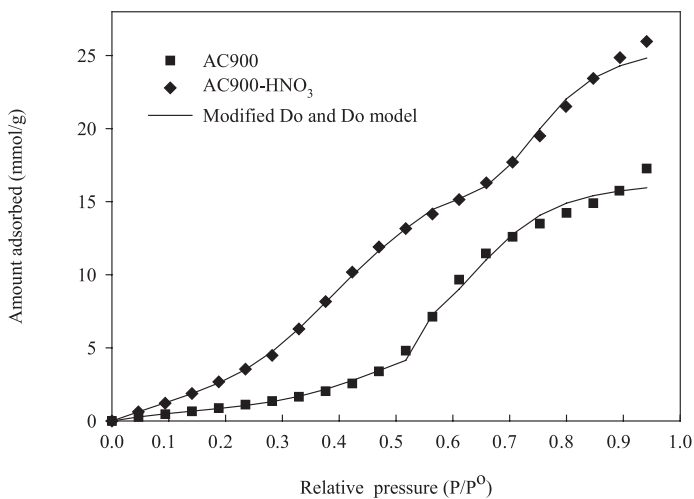


Figure 8. Fitting of the modified Do and Do model to the water vapor adsorption isotherms at 30°C

Table 7. Parameters obtained from the modified Do and Do model

| | S_0 (mmol/g) | K_f | $C_{\mu s}$ (mmol/g) | K_{μ} | n | R^2 |
|------------------------|-------------------|--------|-------------------------|-----------|-----|-------|
| AC900 | | | | | | |
| $P/P^0 \leq 0.5$ | 1.16 | 5.84 | 4.74 | 25.09 | 5 | 0.981 |
| $P/P^0 > 0.5$ | 0.13 | 145.12 | 10.76 | 78.26 | 10 | 0.957 |
| AC900-HNO ₃ | | | | | | |
| $P/P^0 \leq 0.5$ | 5.34 | 2.55 | 7.70 | 88.07 | 5 | 0.999 |
| $P/P^0 > 0.5$ | 0.25 | 8.64 | 9.24 | 79.56 | 15 | 0.985 |

Conclusion

The surface modification of eucalyptus wood-based activated carbon using HNO_3 oxidation was performed to enhance the adsorption capacity of water vapor. Oxidation of the activated carbon surface considerably increases the amount of oxygen attachment in the form of acidic functional groups. The adsorption capacity of water vapor was improved with the presence of oxygen functional groups on the activated carbon surfaces. The adsorption isotherms of the original and oxidized activated carbons activated at 600°C were well fitted by the original Do and Do model. The cluster model of Do and Do was modified to fit the adsorption isotherms of the original and oxidized activated carbons activated at 900°C , which contained mesopore volume. To obtain good simulation results at relative pressures higher than about 0.5, the number of adsorbed water molecules in the cluster needed to be changed from 5 to 10 and 15 for the original and oxidized activated carbons, respectively.

References

- Biniak, S., Pakula, M., Szymański, G.S., and Świątkowski, A. (1999). Effect of activated carbon surface oxygen- and/or nitrogen-containing groups on adsorption of copper(II) ions from aqueous solution. *Langmuir*, 15(18):6,117.
- Birkett, G.R., and Do, D.D. (2006). The adsorption of water in finite carbon pores. *Molecular Physics*, 104(4):623.
- Cordero, T., Rodriguez-Mirasol, J., Tancredi, N., Piriz, J., Vivo, G., and Rodriguez, J.J. (2002). Influence of surface composition and pore structure on Cr(III) adsorption onto activated carbons. *Ind. Eng. Chem. Res.*, 41(24):6,042.
- Do, D.D. (1998). *Adsorption analysis: Equilibria and kinetics*. Imperial College Press, Singapore, p. 77-88.
- Do, D.D., and Do, H.D. (2000). A model for water adsorption in activated carbon. *Carbon*, 38(5):768.
- Dubinin, M.M., and Serpinsky, V.V. (1981). Isotherm equation for water vapor adsorption by microporous carbonaceous adsorbents. *Carbon*, 19(5):402.
- El-Hendawy, A.-N.A. (2003). Influence of HNO_3 oxidation on the structure and adsorptive properties of corn-cob-based activated carbon. *Carbon*, 41(4):713.
- Girgis, B.S., Yunis, S.S., and Soliman, A.M. (2002). Characteristics of activated carbon from peanut hulls in relation to conditions of preparation. *Materials Letters*, 57(1):164.
- Gomez-Serrano, V., Pastor-Villegas, J., Duran-Valle, C.J., and Valenzuela-Calahorra, C. (1996). Heat treatment of rockrose char in air. Effect on surface chemistry and porous texture. *Carbon*, 34(4):533.
- Harding, A.W., Foley, N.J., Norman, P.R., Francis, D.C., and Thomas, K.M. (1998). Diffusion barriers in the kinetics of water vapor adsorption/desorption on activated carbons. *Langmuir*, 14(14):3,858.
- Haydar, S., Ferro-García, M.A., Rivera-Utrilla, J., and Joly, J.P. (2003). Adsorption of *p*-nitrophenol on an activated carbon with different oxidations. *Carbon*, 41(3):389.
- Jagtøyen, M., and Derbyshire, F., (1998). Activated carbon from yellow poplar and white oak by H_3PO_4 activation. *Carbon*, 36(7-8):1,085.
- Jiang, Z., Liu, Y., Sun, X., Tian, F., Sun, F., Liang, C., You, W., Han, C., and Li, C. (2003). Activated carbons chemically modified by concentrated H_2SO_4 for the adsorption of pollutants from wastewater and dibenzothiophene from fuel oils. *Langmuir*, 19:731.
- Junpirom, S., Tangsathitkulchai, C., Tangsathitkulchai, M., and Ngernyen, Y. (2006). Water adsorption in activated carbons with different burn-offs and its analysis using the cluster model, in preparation.
- Lastoskie, C., Gubbins, K.E., and Quirke, N. (1993). Pore size distribution analysis of microporous carbons: a density functional theory approach. *J. Phys. Chem.*, 97(18): 4,786.
- McCallum, C.L., Bandosz, T.J., McGrother, S.C., Müller, E.A., and Gubbins, K.E. (1999).

- A molecular model for adsorption of water on activated carbon: Comparison of simulation and experiment. *Langmuir*, 15(2):533.
- Moreno-Castilla, C., López-Ramón, M.V., and Carrasco-Marín, F. (2000). Changes in surface chemistry of activated carbons by wet oxidation. *Carbon*, 38(14):1,995.
- Müller, E.A., Rull, L.F., Vega, L.F., and Gubbins, K.E. (1996). Adsorption of water on activated carbons: A molecular simulation study. *J. Phys. Chem.*, 100(4):1,189.
- Ngernyen, Y., Tangsathikulchai, C., and Tangsathikulchai, M. (2006). Porous properties of activated carbon produced from eucalyptus and wattle wood by carbon dioxide activation. *Korean J. Chem. Eng.*, 23(6):1,046.
- Olivier, J.P. (1995). Modeling physical adsorption on porous and nonporous solids using density functional theory. *J. of Porous Materials*, 2:9.
- Rivera-Utrilla, J., and Sánchez-Polo, M. (2003). Adsorption of Cr(III) on the ozonised activated carbon. Importance of $C\pi$ -cation interactions. *Water Research*, 37 (14):3,335.
- Rouquerol, F., Rouquerol, J., and Sing, K. (1999). Adsorption by Powders and Porous Solids. Academic Press, London, p. 277-279.
- Salame, I.I., and Bandosz, T.J. (1999). Study of water adsorption on activated carbons with different degrees of surface oxidation. *J. Coll. Int. Sci.*, 210(2):367.
- Salame, I.I., and Bandosz, T.J. (2000). Adsorption of water and methanol on micro- and mesoporous wood-based activated carbons. *Langmuir*, 16(12): 5,435.
- Salame, I.I., and Bandosz, T.J. (2001). Surface chemistry of activated carbons: Combining the results of temperature-programmed desorption, Boehm, and Potentiometric titrations. *J. Coll. Int. Sci.*, 240(1):256.
- Salame, I.I., and Bandosz, T.J. (2003). Role of surface chemistry in adsorption of phenol on activated carbons. *J. Coll. Int. Sci.*, 264(2):308.
- Strelko, Jr.V., Malik, D.J., and Streat, M. (2002). Characterisation of the surface of oxidised carbon adsorbents. *Carbon*, 40(1):95.
- Vagner, C., Fingueneisel, G., Zimny, T., and Weber, J.V. (2002). Water vapour adsorption on activated carbons: comparison and modeling of the isotherms in static and dynamic flow conditions. *Fuel Processing Technology*, 77-78:409.